Capacitance Computation for CPW Discontinuities with Finite Metallization Thickness by Hybrid Finite-Element Method

Chien-Wen Chiu and Ruey-Beei Wu, *Member, IEEE*

***Abstract*—A variational equation is derived for the capacitances of coplanar waveguide (CPW) structures with finite metallization thickness. The equation is expressed in terms of the static potential in the slot region and is solved by applying the hybrid finite-element method (FEM). In case of small metallization thickness, it is reduced to a perturbation formula for the incremental capacitances. Numerical results for the equivalent capacitances of various discontinuities with finite metallization thickness are presented and compared with measured data. The reasonable agreement between the measured data and the theoretical results validates the present approach. Being simple and computationally efficient, the method is suitable to deal with extensive CPW discontinuity problems where the metallization thickness is not negligible.**

***Index Terms*— Capacitance, coplanar waveguides, finite-element method (FEM), transmission-line discontinuities.**

I. Introduction

THE COPLANAR waveguide (CPW), which offers some advantages over the conventional microstrip line, has become an alternate in the design of monolithic microwave integrated circuit (MMIC) devices. Its planar dimension can be shrunken substantially while maintaining the propagation characteristics, which depend mainly on the strip-to-slot-width ratio. Comparatively, the effects of the metallization thickness are not negligible and should be taken into account. As submicron IC technology develops, it will soon become common that the metallization thickness is comparable to, or even larger than, the width.

Recently, several papers have been presented to characterize CPW discontinuity structures with finite metallization thickness [1]–[6]. Although able to include some dispersive characteristics of CPW discontinuities, these full-wave methods are, in general, quite time consuming. As a result, the numerical analysis does not allow sufficient cell division for satisfactory convergency. Moreover, the calculated results reveal that the dispersion of CPW structures is much smaller than that of the microstrip. By a survey of the literature, it is found that the error due to the neglect of dispersion is, in general, smaller than 5% over the frequency band up to 70 GHz for common CPW structures with a line dimension smaller than 100 μm [3], [7]–[9]. Ironically, there are examples showing that insufficient cell division and poor convergency in the full-wave analyses may result in larger error than the negligence of dispersion in the quasi-static approximation.

Being direct in extracting element values of equivalent circuit models, analyses based on the quasi-static approximation have been employed to deal with CPW discontinuities. Naghed *et al.* applied the three-dimensional (3-D) finite difference method (FDM) to calculate equivalent capacitances and inductances of various CPW discontinuities [10], [11]. The FDM calls for the solution of the field distribution at the grid points of the 3-D space such that it may exhaust the available computation memory but still have an insufficient amount of resolution to model the field in the slot region, which is of essential concern. To alleviate the computation load, a new methodology which requires only the solution for the field distribution on the slot aperture of the metallization plane was proposed to calculate the capacitances and inductances of CPW structures with zero thickness [12], [13]. Being very economical in memory usage, it allows an increase of the resolution in mesh division until satisfactory convergence has been reached. The methodology has been found very successful in the design and simulation of complicated CPW circuits, such as bandpass filters [14].

This paper generalizes the methodology to the capacitance computation for CPW structures with finite metallization thickness. The variational equation in terms of the scalar potential distribution in the slot region is derived in Section II. It is solved by applying the hybrid finite-element method (FEM). In the case of small metallization thickness, the equation is reduced to a simple perturbation formula for the incremental capacitances in Section III. The hybrid FEM is applied to deal with uniform CPW and open-end discontinuity in Section IV. The results are compared with those predicted by the perturbation formula to depict the applicable range of the perturbation analysis. Numerical results for extensive CPW discontinuities based on the perturbation formula are presented in Section V. Finally, brief conclusions are drawn in Section VI.

II. Variational Equation for CPW Capacitance

Fig. 1 shows the cross section of CPW structures with finite conductor thickness t. Under the quasi-static model, the CPW

Manuscript received March 18, 1996; revised December 24, 1996. This work was supported in part by the National Science Council, Republic of China, under Grant NSC85-2221-E002-022.

C.-W. Chiu is with the Department of Electronic Engineering, Jin-Wen College of Business and Technique, Taiwan, R.O.C.

R.-B. Wu is with the Department of Electrical Engineering, National Taiwan University, Taipei, Taiwan, R.O.C.

Publisher Item Identifier S 0018-9480(97)02530-1.

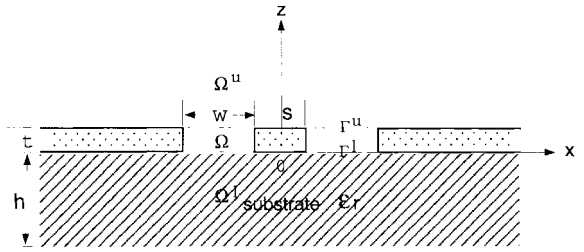

Fig. 1. Cross section of CPW structures with finite metallization thickness t.

capacitance C can be found from the total stored electrical energy W_e in the whole space. It is a variational formula for capacitance $C = 2W_e/V^2 = 2W_e$ if a unit voltage drop is impressed between the central signal strip and grounds.

Consider a general 3-D CPW discontinuity structure with the cross section shown in Fig. 1. The whole space can be divided into the upper space Ω^u, the lower space Ω^l, and the slot region Ω. The total electric energy W_e is

$$W_e = W_e^u + W_e^l + \frac{1}{2}\int_\Omega \epsilon \vec{E}\cdot\vec{E}\ \ d\Omega \tag{1}$$

where W_e^u and W_e^l are the electric energy stored in the upper and lower regions, respectively.

Introducing a vector electric potential $\vec{A_e}$ and following a similar derivation procedure in [12], the stored energy W_e^u and W_e^l can be related to the scalar potential on the slot apertures Γ^u and Γ^l by [12, eq. (7)]. Hence, the total electric energy can be expressed in terms of the scalar potential $\phi(\vec{\rho},z),\ 0 \le z \le t$, by

$$\begin{aligned} W_e = {} & \frac{1}{2}\int_{\Gamma^u}\int_{\Gamma^u} G^u(\vec{\rho};\vec{\rho}')\bigtriangledown_\rho \phi(\vec{\rho},z=t) \\ & \cdot \bigtriangledown_{\rho'}\phi(\vec{\rho}',z'=t)d\Gamma\, d\Gamma' \\ & + \frac{1}{2}\int_{\Gamma^l}\int_{\Gamma^l} G^l(\vec{\rho};\vec{\rho}')\bigtriangledown_\rho \phi(\vec{\rho},z=0) \\ & \cdot \bigtriangledown_{\rho'}\phi(\vec{\rho}',z'=0)\, d\Gamma d\Gamma' \\ & + \frac{1}{2}\int_\Omega \epsilon \bigtriangledown \phi(\vec{\rho},z)\cdot\bigtriangledown\phi(\vec{\rho},z)d\Omega \end{aligned} \tag{2}$$

where G^u and G^l are the space-domain Green's function for the upper and lower spaces, respectively [12], and $\vec{\rho}$ denotes the position vector in the x-y plane.

It is well known that the variational equation (2) can be solved by applying the Ritz procedure. Consider a general 3-D structure with the cross section shown in Fig. 1. In applying the Ritz procedure, the first step is to choose a basis for the unknown potential distribution $\phi(x, y, z)$. In the light of the FEM [15], the solution region is divided into a lot of small rectangular prisms, the so-called finite elements. The potential distribution $\phi(x, y, z)$ over each element, say the one shown in Fig. 2, can be modeled as a linear combination of first-order shape functions. For example, the first-order shape function for node 1 shown in Fig. 2 is

$$f_1(x,y,z) = \left(\frac{1}{2}+\frac{x-x_o}{\triangle_x}\right)\left(\frac{1}{2}+\frac{y-y_o}{\triangle_y}\right)\left(\frac{1}{2}+\frac{z-z_o}{\triangle_z}\right). \tag{3}$$

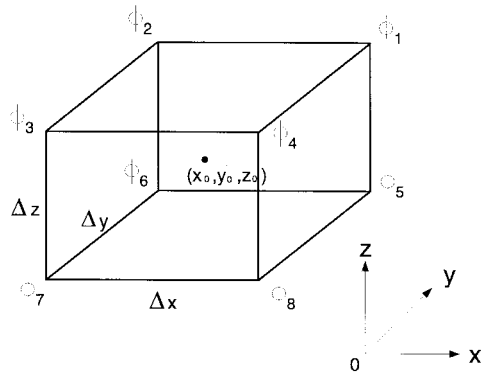

Fig. 2. A typical element used for scalar potential modeling.

Note that this shape function takes on value 1 at node 1, and 0 at all other nodes. Then, over this element ($|x-x_o| \le \frac{1}{2}\triangle_x,\ |y-y_o| \le \frac{1}{2}\triangle_y,\ |z-z_o| \le \frac{1}{2}\triangle_z$), $\phi(x,y,z)$ is defined as

$$\phi(x,y,z) = \sum_{n=1}^{8} f_n(x,y,z)\phi_n. \tag{4}$$

It deserves mentioning that the present approach can be applied to deal with complicated CPW discontinuities of arbitrary shape. One need only employ more general hexahedral elements, for which the shape functions are available in textbooks on FEM, (e.g., [16]).

Substituting (4) into (2), the Ritz procedure is applied for solving the variational equation for the unknown nodal values ϕ_n's. As the impressed voltage is known at the nodes on the boundary of the slot regions, the internal node ϕ_i, and then the capacitance, can be obtained from that equation. Thus, the equivalent capacitance of CPW discontinuity can be extracted.

III. Perturbation Analysis

Although capable of treating CPW structures with finite metallization thickness, the hybrid FEM analysis for solving the 3-D $\phi(\vec{\rho},0 \le z \le t)$ is numerically intensive. The time-consuming analysis is not indispensable in tackling those complicated 3-D problems.

In some MMIC applications, the thickness t is small, though not negligible as compared with the slot width. Treating it as a perturbation, the capacitance can be written as $C = C_0 + tC_1$, where C_0 is the capacitance obtained at a zero-thickness limit. That is,

$$\begin{aligned} C_0 = {} & \int_\Gamma\int_\Gamma \left[G^u(\vec{\rho};\vec{\rho}') + G^l(\vec{\rho};\vec{\rho}')\right]\bigtriangledown_\rho \phi_0(\vec{\rho}) \\ & \cdot \bigtriangledown_{\rho'}\phi_0(\vec{\rho}')\, d\Gamma\, d\Gamma' \end{aligned} \tag{5}$$

where $\Gamma^u \to \Gamma^l \equiv \Gamma$ as $t \to 0$ and $\phi_0(\vec{\rho})$ denotes the scalar potential on the slot surface in the zero-thickness limit. C_1 denotes the per-unit-thickness incremental capacitance due to the stored energy in the slot region. It can be expressed as

$$C_1 = \int_\Gamma \epsilon \bigtriangledown_\rho \phi_0 \cdot \bigtriangledown_\rho \phi_0 d\Gamma + \int_\Gamma \epsilon \frac{\partial\phi_0}{\partial z}\frac{\partial\phi_0}{\partial z}d\Gamma. \tag{6}$$

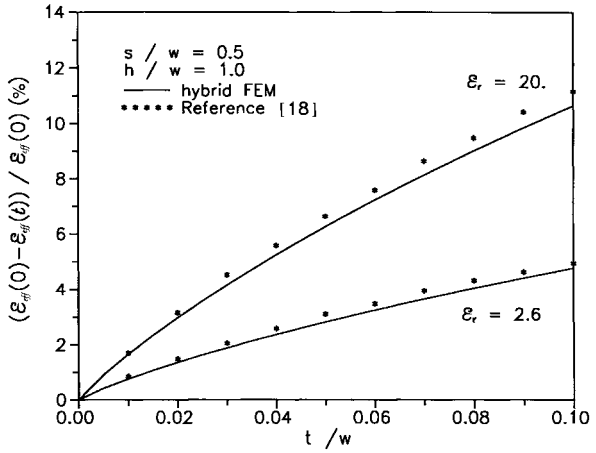

Fig. 3. Effect of finite metallization thickness on the effective dielectric constant ϵ_{eff}. Comparison between the calculated results (the solid curves) and those in [18] (cross points).

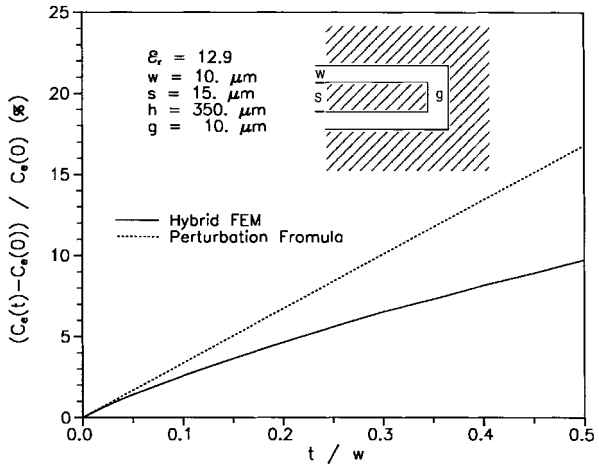

Fig. 5. The incremental equivalent capacitance ratio of open-end discontinuity versus t/w.

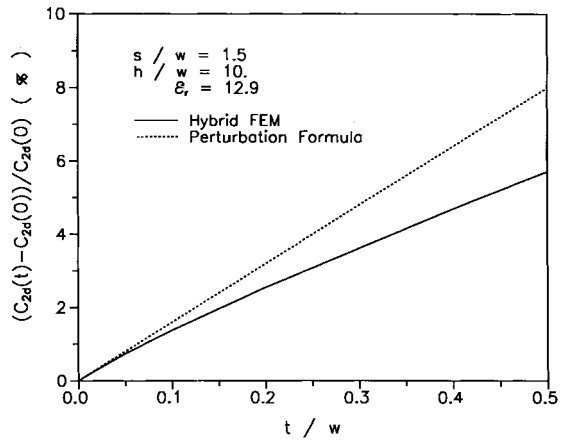

Fig. 4. The incremental capacitance ratio of a uniform CPW versus metallization thickness t/w.

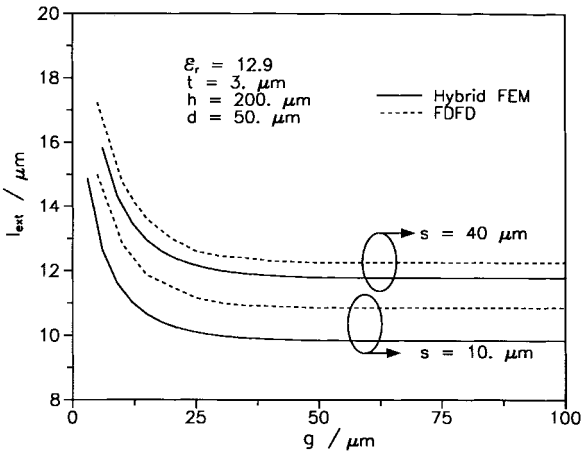

Fig. 6. Calculated effective length extension of open-end CPW by quasi-static approximation as compared to those by FDFD [3] with metallization thickness $t = 3$ μm.

The Ritz procedure can be applied toward solving the variational equation (5) for the unknown scalar potential $\phi_0(\vec{\rho})$ and the capacitance C_0 [12]. Note that $\phi_0(\vec{\rho})$ is a two-dimensional (2-D) field and the numerical solution is much simpler. Then, $\phi_0(\vec{\rho})$ could be used to directly evaluate the incremental capacitance C_1 by (6). Numerical analyses for uniform CPW transmission-line and open-end discontinuity show that the second term in the right side of (6) is negligible as compared with the first term. Finally, the equivalent capacitances of CPW structures with finite metallization thickness could be estimated from the perturbation formula $C = C_0 + tC_1$.

IV. Numerical Results for Hybrid FEM and Perturbation Formula

In the numerical computation, the mesh division is chosen to be nonuniform in both x- and y-directions using the sinusoidal scheme [17], while uniform in the z-direction. Numerical tests have been conducted by increasing the number of cells in each direction to assure that satisfactory convergency has been achieved. Fig. 3 shows the effects of finite metallization thickness on the effective dielectric constant $\epsilon_{\text{eff}}(t)$ of a uniform CPW. The results by the hybrid FEM are presented and compared with those in [18]. Agreement between these results is observed with some difference. This difference may be contributed to the inaccurate modeling for the singularities of the field near the edge in both methods and the slow convergence of the series expression for the Green's function in [18].

Fig. 4 shows the incremental capacitance ratio of a uniform CPW versus t/w with s/w as a parameter. The solid and dashed curves stand for the results obtained by the finite element and perturbation analyses, respectively. It is worth noting that the contribution of the second term in the right-hand side (RHS) of (6) can be neglected since the longitudinal component of the electric field is much smaller than the transverse component. In the case of thick metallization, the incremental capacitance tends to be that between the two parallel sides of the slot. The propagation characteristics are hybrid of the CPW and parallel plate modes. In the case of small metallization thickness, say $t/w \leq 0.15$, the perturbation analysis is found to yield satisfactory results and the error lies below 0.5% of C_0.

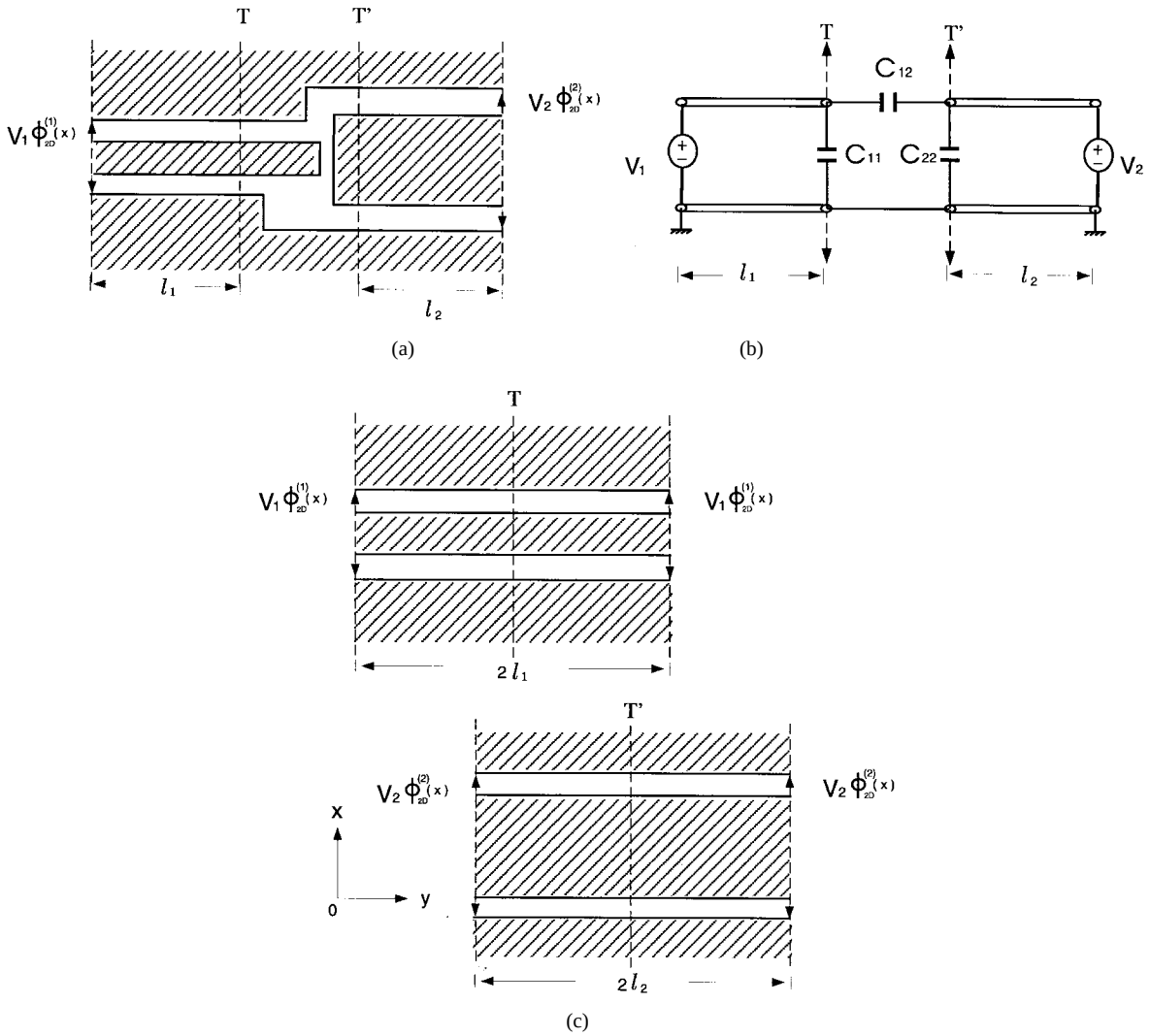

Fig. 7. (a) Metallization plane of a typical CPW discontinuity. (b) Its equivalent capacitance circuit, and (c) two auxiliary structures.

Fig. 5 shows the incremental capacitance ratio of an open-end discontinuity versus t/w with central conductor width s and gap width g as parameters. The extraction scheme for the equivalent capacitance of open-end discontinuity from the 3-D capacitance can be referred to in [12]. The calculated results show that the increment of the open-end capacitance due to metallization thickness is below 10% in a MMIC structure. In case of thickness ratio $t/w = 0.15$, the increment is about 3.5%. It is found that the effect of finite metallization thickness on the equivalent capacitance is not significant and can be approximately evaluated by using the perturbation formula in typical MMIC cases.

Fig. 6 compares the results based on the hybrid FEM and those by using the finite difference frequency domain (FDFD) method [3]. The equivalent length extension of an open-end discontinuity is defined as C_e/C_{2d} where C_{2d} is the transmission-line capacitance of uniform CPW. The results by these two method exhibit a similar tendency, but the comparison shows a noticeable discrepancy. This discrepancy may be partly due to the error in extracting the capacitances by using the FDM. It has been recently demonstrated that the capacitance calculated by the FDM with a reasonable-sized grid may be of considerable error. For example, Table I compares the characteristic impedance of uniform CPW calculated by a conventional FDM, improved FDM, conformal mapping method (CMM) and the present FEM, where the FDM results are extracted from [19, Figs. 4 and 5]. The error of the results obtained by conventional FDM employed in [3] is found to be 10%–20% (i.e., the same order of that depicted in Fig. 6).

TABLE I
COMPARISON OF CPW CHARACTERISTIC IMPEDENCE CALCUALTED BY FDM, CMM, AND THE PRESENT FEM

Thickness	FDM	Improved FDM	CMM	FEM
$t = 0$	46.01	48.20	49.74	49.65
$t = 3$	41.35	42.65	44.00	43.73

$s = 15\ \mu$m, $\epsilon_r = 12.9$, $h = 200\ \mu$m

V. COMPUTATION FOR VARIOUS CPW DISCONTINUITIES

In case of small metallization thickness, e.g. $t/w \leq 0.15$, the variational equation (5) at the zero thickness limit can be easily applied to solve the CPW discontinuity with more complicated

geometric configuration. Then, (6) is used to predict the finite metallization thickness effect. The approach is useful and beneficial to deal with general CPW discontinuities which have more than one output port. However, the extraction scheme for the equivalent capacitance is different from that proposed in [12]. It is briefly described as follows.

Consider a general CPW discontinuity structure shown in Fig. 7(a). To facilitate the analysis, the discontinuity is assumed to be connected to two ports of uniform CPW's which are of lengths l_1 and l_2, respectively. As the length becomes large, the electric potential distribution $\phi(\vec{\rho})$ at the two truncated ends will tend to be proportional to that of infinitely extending uniform CPW's, (i.e., $\phi_{2D}^{(1)}(x)$ and $\phi_{2D}^{(2)}(x)$). Let the voltages imposed on the two CPW's be V_1 and V_2, the electric potential $\phi(\vec{\rho})$ on the slot apertures will satisfy the variational equation

$$W_e(l_1;l_2)=\frac{1}{2}\int\!\!\int_S\int\!\!\int_S G(\vec{\rho};\vec{\rho}')\,\nabla_t\,\phi(\vec{\rho})\cdot\nabla_{t'}\phi(\vec{\rho}')dS'dS \tag{7}$$

subject to the boundary conditions that $\phi(\vec{\rho})$ equals $V_1\cdot\phi_{2D}^{(1)}(x)$ and $V_2\cdot\phi_{2D}^{(2)}(x)$ at the two truncated ends.

According to the equivalent circuit shown in Fig. 7(b), the stored electric energy W_e in (7) can be written as

$$\begin{aligned}W_e=&\frac{1}{2}V_1^2\left(l_1\cdot C_{2D}^{(1)}+C_{\text{end}}^{(1)}+C_{11}\right)\\&+\frac{1}{2}V_2^2\left(l_2\cdot C_{2D}^{(2)}+C_{\text{end}}^{(2)}+C_{22}\right)+\frac{1}{2}C_{12}(V_1-V_2)^2\end{aligned} \tag{8}$$

where $C_{2D}^{(i)}(i=1,2)$ is the per-unit length capacitance of the ith CPW and $C_{\text{end}}^{(i)}$ is included to model the contribution due to the truncated end where the source V_i applies. To eliminate the undesired $C_{\text{end}}^{(i)}$, two auxiliary structures shown in Fig. 7(c) are considered. Each structure consists of a uniform CPW with finite length $2l_i$ $(i=1,2)$. Applying (7) to the two auxiliary structures can solve the electric potential distribution and yield the stored electric energy

$$W_e^{(i)}(2l_i)=\frac{1}{2}V_i^2\left(C_{\text{end}}^{(i)}\cdot 2+2l_i\cdot C_{2D}^{(i)}\right),\qquad i=1,2. \tag{9}$$

Subtracting (9) from (8) de-embeds the two CPW sections and gives a realization of the desired equivalent capacitances, i.e.,

$$\begin{aligned}&C_{11}V_1^2+C_{22}V_2^2+C_{12}(V_1-V_2)^2\\&\quad=\lim_{l_1,l_2\to\infty}[2W_e(l_1;l_2)-W_e^{(1)}(2l_1)-W_e^{(2)}(2l_2)].\end{aligned} \tag{10}$$

If the imposed voltages (V_1, V_2) are chosen as (1,0), (0,1), and (1,1), the obtained values from (7) will be $C_{11}+C_{12}, C_{22}+C_{12}$ and $C_{11}+C_{22}$, respectively. The desired equivalent capacitances C_{11}, C_{22}, and C_{12} can thus be obtained.

The above procedure can be applied to deal with more general discontinuity structures with multiple ports. For a discontinuity structure with N ports, there are $\frac{1}{2}N(N+1)$ equivalent capacitances $C_{ij}(i,j=1,2,\cdots,N)$. They can be solved from $\frac{1}{2}N(N+1)$ realizations by choosing $\frac{1}{2}N(N+1)$ independent combinations of the imposed voltages.

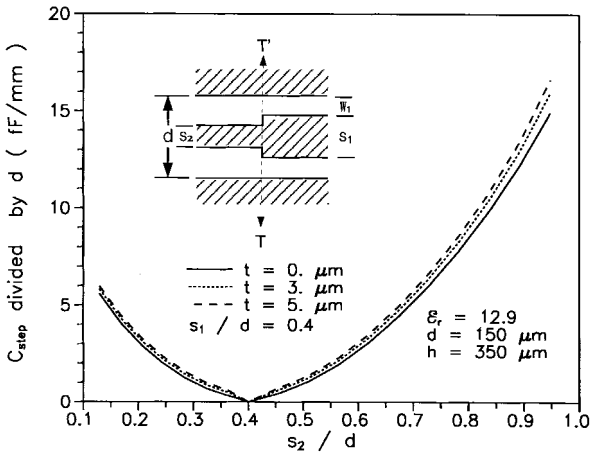

Fig. 8. Calculated equivalent capacitances of symmetric step change divided by total linewidth d versus s_2/d with t as a parameter.

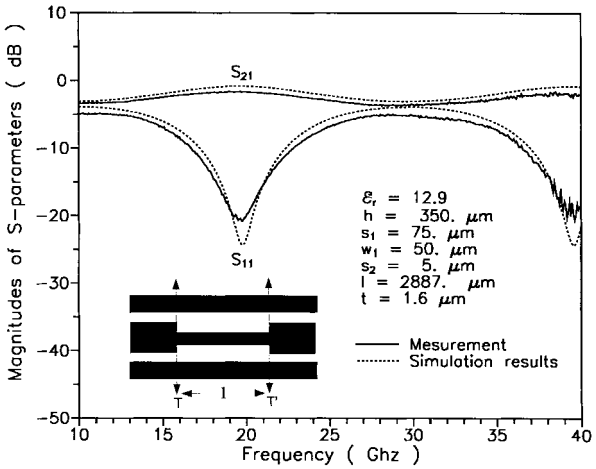

Fig. 9. Measured S-parameters are compared with the simulation results for the double step-change.

Fig. 8 shows the equivalent capacitance of a symmetric step change in width versus s_2/d with t as a parameter. The present structure is a two-port capacitance system and the equivalent π circuit is applied. Here, the two ports must have the same voltage $V_1=V_2$ such that the shunt capacitance is given by $C_{\text{step}}=C_{11}+C_{22}$. For typical MMIC configurations with the total linewidth in the order of 100 μm, the shunt capacitance is about several fF. The shunt capacitance tends to zero as s_2 tends to s_1.

Fig. 9 shows the measured S-parameters for the double-step change. The capital letters T and T' denote the reference planes at which the measurement is performed. The measurement is performed on a Cascade Microtech probe station using an HP8510 network analyzer based on the thru-reflection-line (TRL) calibration technique. The authors chose $l=2.887$ mm so that the resonance frequency for the minimum reflection coefficiency is about 20 GHz. The dotted lines also shown in the figure are the results simulated by the EEsof[1] package. In the simulation, the step change is modeled by a symmetric lumped π-model which includes series inductance [13] and shunt capacitance obtained by the present approach. The CPW

[1] EEsof is a trademark of Hewlett Packard software.

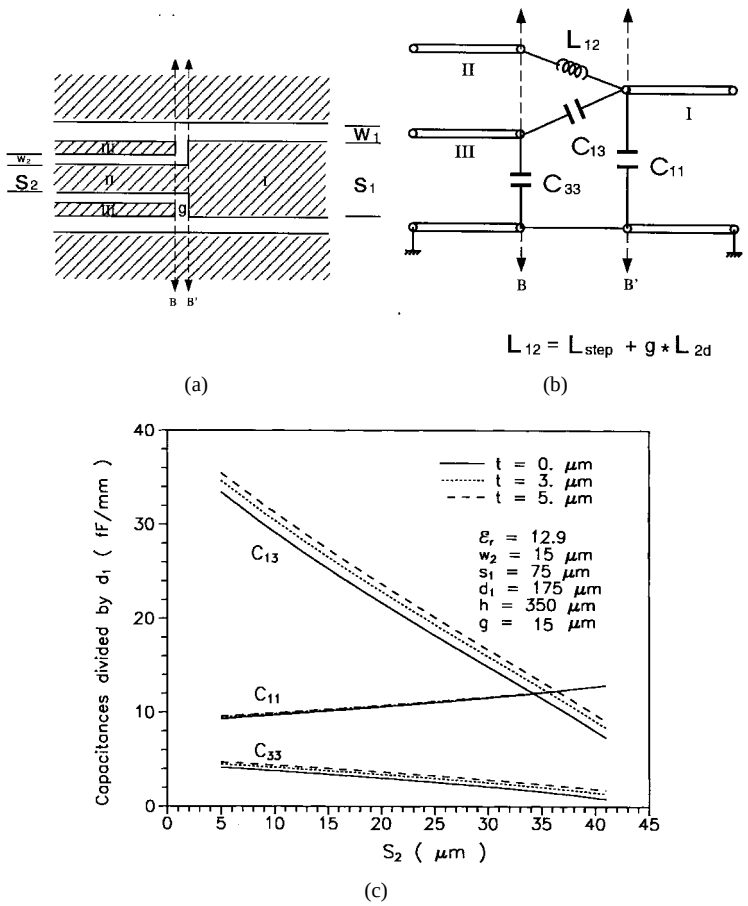

Fig. 10. (a) Complicated edge coupled stub structure in conventional CPW configuration, (b) its equivalent circuit model, and (c) calculated equivalent capacitances divided by the total linewidth d_1 versus the strip width s_2 with s_1, w_1, and w_2 as parameters.

section is modeled by a transmission line with attenuation constant α being about 0.2196 dB/mm at 20 GHz, which is extracted from the measured data in the TRL calibration. It is found that the simulation results can predict the frequency response satisfactorily.

The same approach can be employed to deal with other more complicated CPW discontinuities. For example, consider a complicated edge-coupled stub shown in Fig. 10(a). The structure is useful in the filter application [14]. The equivalent circuit of discontinuity can be constructed as Fig. 10(b), which includes three equivalent capacitances. Fig. 10(c) shows the calculated results versus the parameters s_2 with t as a parameter but with total linewidth of the structure $d_1 = s_1 + 2w_1$ fixed. Due to the choice of reference planes, C_{11} is comparable to C_{13} since it includes the contributions from both the discontinuity and a transmission-line section of length g. On the contrary, C_{33} is far smaller than C_{13} and could be omitted in the circuit design. The quasi-static circuit model has been applied in the design and simulation of a ribbon-of-brick-wall (RBW) filter and the results are in good agreement with the measured data [14].

VI. Conclusion

In this paper, variational equations for the 2-D and 3-D capacitances for the CPW's with finite metallization thickness are employed and subsequently solved by applying the hybrid FEM. In case of small metallization thickness, the equations can be reduced to the perturbation formula, which is much more numerically efficient. From the comparison with the results by the FEM, it is found that the error due to the perturbational analysis lies below 1.5% for typical MMIC structures with thickness-to-linewidth ratio $t/w \leq 0.15$. The perturbation formula is then extended to deal with more complicated CPW discontinuity problems. Numerical results for the equivalent capacitances of various discontinuities have been presented and compared with measured data. The obtained equivalent circuit based on the quasi-static analysis is applicable up to millimeter-wave frequency range for practical CPW discontinuity structures in MMIC's.

References

[1] C. W. Kuo and T. Itoh, "Characterization of shielded coplanar type transmission line junction discontinuities incorporating the finite metallization thickness effect," *IEEE Trans. Microwave Theory Tech.*, vol. 40, pp. 73–80, Jan. 1992.

[2] T. W. Huang and T. Itoh, "The influence of metallization thickness on the characteristics of cascaded junction discontinuities of shielded coplanar type transmission line," *IEEE Trans. Microwave Theory Tech.*, vol. 41, pp. 693–697, Apr. 1993.

[3] K. Beilenhoff, H. Klingbeil, W. Heinrich, and H. L. Hartnagel, "Open and short circuits in coplanar MMIC's," *IEEE Trans. Microwave Theory Tech.*, vol. 41, pp. 1534–1537, Sept. 1993.

[4] A. M. Tran and T. Itoh, "Full-wave modeling of coplanar waveguide discontinuities with finite conductor thickness," *IEEE Trans. Microwave Theory Tech.*, vol. 41, pp. 1611–1615, Sept. 1993.

[5] F. Alessandri, G. Baini, M. Mongiardo, and R. Sorrentino. "A 3-D mode matching technique for the efficient analysis of coplanar MMIC discontinuities with finite metallization thickness," *IEEE Trans. Microwave Theory Tech.*, vol. 41, pp. 1625–1629, Sept. 1993.
[6] R. Schmidt and P. Russer, "Modeling of cascaded coplanar waveguide discontinuities by the mode-matching approach," in *IEEE MTT-S Int. Microwave Symp. Dig.*, Orlando, FL, May 1995, pp. 281–284.
[7] W. Heinrich, "Quasi-TEM description of MMIC coplanar lines including conductor loss effects," *IEEE Trans. Microwave Theory Tech.*, vol. 41, pp. 45–52, Jan. 1993.
[8] S. Bedair and I. Wolff, "Fast, accurate, and simple approximate analytic formula for calculating the parameters of supported coplanar waveguides," *IEEE Trans. Microwave Theory Tech.*, vol. 40, pp. 41–48, Jan. 1992.
[9] N. I. Dib and L. P. B. Katehi, "Modeling of shielded CPW discontinuities using the space domain integral equation method," *J. Electromagnetic Waves Applicat.*, vol. 5, pp. 503–523, 1991.
[10] M. Naghed and I. Wolff, "Equivalent capacitances of coplanar waveguide discontinuities and interdigitated capacitors using a three-dimensional finite difference method," *IEEE Trans. Microwave Theory Tech.*, vol. 38, pp. 1808–1815, Dec. 1990.
[11] M. Naghed, M. Rittweger, and I. Wolff, "A new method for the calculation of the equivalent inductances of coplanar waveguide discontinuities," in *IEEE MTT-S Int. Microwave Symp. Dig.*, Boston, MA, June 1991, pp. 747–750.
[12] M. H. Mao, R. B. Wu, C. H. Chen, and C. H. Lin, "Characterization of coplanar waveguide open end capacitance—Theory and experiment," *IEEE Trans. Microwave Theory Tech.*, vol. 42, pp. 1016–1024, June 1994.
[13] C. W. Chiu and R. B. Wu, "A moment method analysis for coplanar waveguide discontinuity inductances," *IEEE Trans. Microwave Theory Tech.*, vol. 41, pp. 1511–1514, Sept. 1993.
[14] F. L. Lin, C. W. Chiu, and R. B. Wu, "Coplanar waveguide bandpass filter—A ribbon-of-brick-wall design," *IEEE Trans. Microwave Theory Tech.*, vol. 43, pp. 1589–1596, July 1995.
[15] T. Itoh, Ed., *Numerical Techniques for Microwave and Millimeter-Wave Passive Structures*. New York: Wiley, 1989, ch. 2.
[16] S. S. Rao, Ed. *The Finite Element Method in Engineering.* New York: Pergamon, 1982, ch. 4, sec. 4.3.6.
[17] W. T. Weeks, "Calculation of coefficients of capacitance of multiconductor transmission lines in the presence of a dielectric interface," *IEEE Trans. Microwave Theory Tech.*, vol. MTT-18, pp. 35–43, Jan. 1970.
[18] T. Kitazawa and Y. Hayashi, "Quasistatic characteristics of a coplanar waveguide with metal coating," *Proc. Inst. Elect. Eng.*, vol. 133, pt. H, pp. 18–20, Feb. 1986.
[19] K. Beilenhoff and W. Heinrich, "Treatment of field singularities in the finite-difference approximation," in *IEEE MTT-S Int. Microwave Symp. Dig.*, Atlanta, GA, June 1993, pp. 979–982.

Chien-Wen Chiu was born in Maoli, Taiwan, R.O.C., in 1962. He received the B.S. degree from National Taiwan Normal University, Taipei, Taiwan, the M.S. and Ph.D. degrees in electrical engineering from National Taiwan University, Taipei, Taiwan, R.O.C., in 1985, 1990, and 1996, respectively.

From 1990 to 1991, he was a member of the Computer and Communication Research Laboratory, where his primary work was on the research and development for Digital European Cordless Telephone. In 1992, he joined the Department of Electronic Engineering, Jin-Wen College of Business and Technique, where he is currently an Associate Professor. His research interests include electromagnetic theory, transmission-line discontinuities.

Ruey-Beei Wu (M'91) was born in Tainan, Taiwan, R.O.C., in 1957. He received the B.S.E.E. and Ph.D. degrees from National Taiwan University, Taipei, Taiwan, R.O.C., in 1979 and 1985, respectively.

In 1982, he joined the faculty of the Department of Electrical Engineering, National Taiwan University, where he is now a Professor. He was a Visiting Scholar at IBM, East Fishkill, NY, from March 1986 to February 1987. From August 1994 to July 1995 he was a Visiting Scholar in the Electrical Engineering Department, University of California, Los Angeles (UCLA). His areas of interest include computational electromagnetics, dielectric waveguides, edge slot antennas, wave scattering of composite materials, transmission line and waveguide discontinuities, and interconnection modeling for computer packaging.